Artificial Organs

Artificial Organs
33(3):250–257, Wiley Periodicals, Inc.
© 2009, Copyright the Authors
Journal compilation © 2009, International Center for Artificial Organs and Transplantation and Wiley Periodicals, Inc.

A Passive Magnetically and Hydrodynamically Suspended Rotary Blood Pump

*†Martin Stoiber, *†Christian Grasl, ‡Stefan Pirker, *Franz Raderer, §Roland Schistek, *†Leopold Huber, ‡Philipp Gittler, and *†Heinrich Schima

**Center for Biomedical Engineering and Physics, Medical University of Vienna; †Ludwig Boltzmann Cluster for Cardiovascular Research, Vienna; ‡Institute of Fluid Mechanics and Heat Transfer, J. Kepler University Linz, Linz; and §Department of Cardiac Surgery, St. John's Hospital, Salzburg, Austria*

Abstract: A combined hydrodynamic–magnetic bearing allows the design of rotary blood pumps that are not encumbered with mechanical bearings and magnets requiring sensors or electrical power. However, such pumps have so far needed very small and accurately manufactured gaps between rotor and housing to assure effective hydromagnetic bearing behavior. In order to use this concept in disposable pump heads, a design that allows larger rotor-housing gaps, and thus larger manufacturing tolerances, is needed. A pump with passive magnetic bearings and a gap between rotor and housing in the range of 0.5 mm was designed. Numerical simulations were performed to optimize the rotor geometry at low levels of shear stress. An experimental test stand was used to find a range of speeds and gap settings that resulted in low levels of vibration and useful pressure–flow relationships. Three different rotor geometries were tested using a viscosity-adjusted test fluid. Blood damage tests were conducted within the desirable range of speeds and gap settings. In this study stable pump performance was demonstrated at total gap widths between 0.3 and 0.7 mm at flows of 0–10 L/min, with afterloads up to 230 mm Hg. Best performance was achieved with rotors sliding on a fluid pillow between the rotor and the outer housing at a gap distance of 50 to 250 µm. The inner gap distance, between the rotor and the inner housing, could be as great as 500 µm. Hemolysis tests on the prototype within the chosen operating range showed lower values (NIH = 0.0029 ± 0.0012 g/100 L) than the Biomedicus BP-80 pump (NIH = 0.0033 ± 0.0011 g/100 L). In conclusion, it is possible to build rotary blood pumps with passive hydromagnetic bearings that have large gaps between their rotors and housings. Rotor behavior is sensitive to the position of the permanent magnetic drive unit. To minimize vibration and blood damage, the fluid gaps and the rotational speed have to be adjusted according to the desired operating point of the pump. Further study is needed to optimize the magnetic drive unit and to ascertain its ability to withstand inertial loads imposed by sudden movements and external shock. **Key Words:** Rotary blood pump—Magnetic levitation—Hydrodynamic levitation—Computational fluid dynamics—Blood trauma.

Magnetically levitated rotary pumps, without mechanical bearings, are leading candidates for improved blood pumping. Rotor levitation can be achieved either by active control of the rotor with electromagnetic actuators, as in the Levitronix Centrimag pump (Levitronix LLC, Waltham, MA, USA), Incor—Berlin Heart (Berlin Heart AG, Berlin, Germany), and the Terumo DuraHeart (Terumo Heart, Inc., Ann Arbor, MI, USA), or by a combination of permanent magnets and hydraulic forces in so-called passive magnetohydrodynamic bearings, as in the Ventrassist (Ventracor, Chatswood, NSW, Australia), the CorAide LVAS (Arrow International, Reading, PA, USA), and the HeartWare (HeartWare, Sydney, NSW, Australia, and Miami, FL, USA) pumps. In these pumps, hydraulic balancing forces are exerted between the housing and a specially shaped rotor. Pumps with passive hydrodynamic bearings do not need electronics with their inherent vulnerability that can lead to failure of sensors and signal leads (1,2).

However, present pumps with passive magnetic bearings require very small gaps between the rotor

doi:10.1111/j.1525-1594.2009.00715.x

Received February 2007; revised September 2008.
Address correspondence and reprint requests to Dr. Martin Stoiber, Center for Biomedical Engineering and Physics, Medical University of Vienna, AKH-4L, Waehringer Guertel 18-20, Vienna A-1090, Austria. E-mail: martin.stoiber@meduniwien.ac.at

Abbott v. Miracor, IPR2025-00116
Miracor Ex. 2022, p. 1 of 8

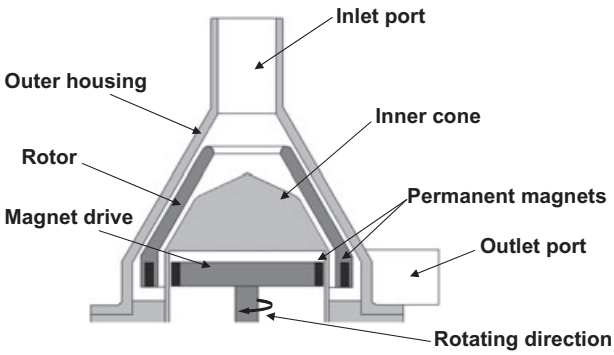

FIG. 1. Schematic cross section of the Hemobear blood pump.

and the housing, and must be manufactured very precisely with low tolerances on the rotor and housing dimensions. For example, the Ventrassist left ventricular assist system incorporates a minimum gap distance of about 50 μm and a total axial clearance of 200 μm (3). Reul and Kink (4) proposed another concept for hydrodynamic blood bearing but it also required very small gaps.

The hemobear blood pump is a diagonal pump (5), driven by an external motor via coupled, passive magnets, with a hydrodynamically suspended rotor. The design permits passive magnetic levitation at comparatively large gaps between the rotor and the housing. These large gaps allow greater manufacturing tolerances and less costly production using injection molding.

MATERIALS AND METHODS

Design of the pump

Figure 1 shows the blood pump in cross section. It has one axial inlet port and, in its current version, two radial outlets that provide a symmetric outflow that balances the load to the rotor. At present, the rotor is driven externally with the rotor and drive coupled by eight pairs of Neodymium Iron Boron magnets. Magnet parameters have not yet been optimized.

The axial position of the permanent magnets on the drive sets the axial position of the rotor. Rotation induces hydrodynamic forces that oppose those from the magnets and stabilize the radial position of the rotor. The axial position is, in the sense of Fig. 1, slightly lower than the no-flow axial rest positions. The vanes of the rotor are specially shaped to propel the blood and to induce these hydrodynamic forces. During operation, the rotor runs free of any contact at a fixed distance from the housing. The pump has a diameter of 55 mm, a height of 50 mm, and diameters of the inlet and outlet ports of 12 and 9 mm, respectively. The priming volume of the pump is 15 mL. Rotational speeds between 2000 and 3000 rpm are possible.

The pump was developed using the computer-aided design (CAD) software package Pro/Engineer Wildfire (PTC Corporation, Needham, MA, USA). A computer-aided manufacturing (CAM) module was used to produce instructions for a five-axis computerized numeric control (CNC) milling machine (PRIMACON, Type PFM 24, Primacon GmbH, Peissenberg, Germany).

Nine different rotor geometries were designed, of which three were tested in this work. The investigated rotor types are shown in Fig. 2. They were formed from polymethyl methacrylate (PMMA). Rotor design A was developed experimentally while rotors B and C were the result of an optimization achieved with numerical simulation. In these rotors, the rounding on the front edge of the vanes was increased from 0.1 to 1 mm.

In the current prototypes, all three rotors are equipped with a thin stabilizing ring to avoid deformation of the vanes by centrifugal forces. In rotors A and B, the stabilizing ring is mounted on one end, farthest from the apex. To effect a better washout, rotor C has the stabilizing ring positioned at mid-height, on the inside of the vanes.

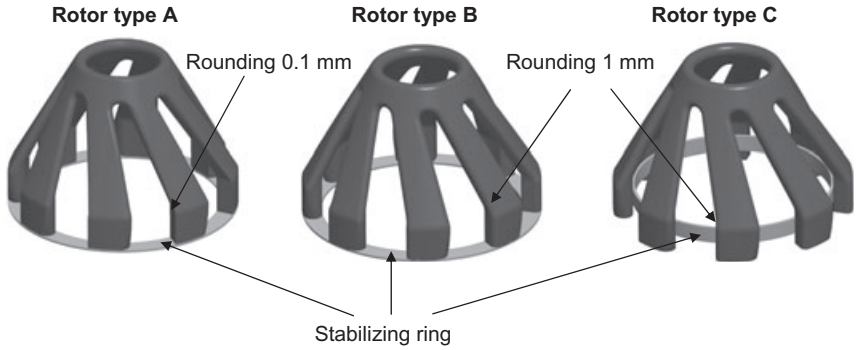

FIG. 2. Rotor designs investigated in this work. Rotor A is the experimentally established design with a 0.1-mm rounding on the front edge. The stabilizing ring is mounted on one end, farthest from the apex. Rotors B and C are the result of an optimization achieved with numerical simulation. In rotor B the rounding on the front edge is increased to 1 mm. In rotor C the rounding on the front edge is increased to 1 mm and the stabilizing ring is placed higher, on the inside of the vanes.

Abbott v. Miracor, IPR2025-00116
Miracor Ex. 2022, p. 2 of 8

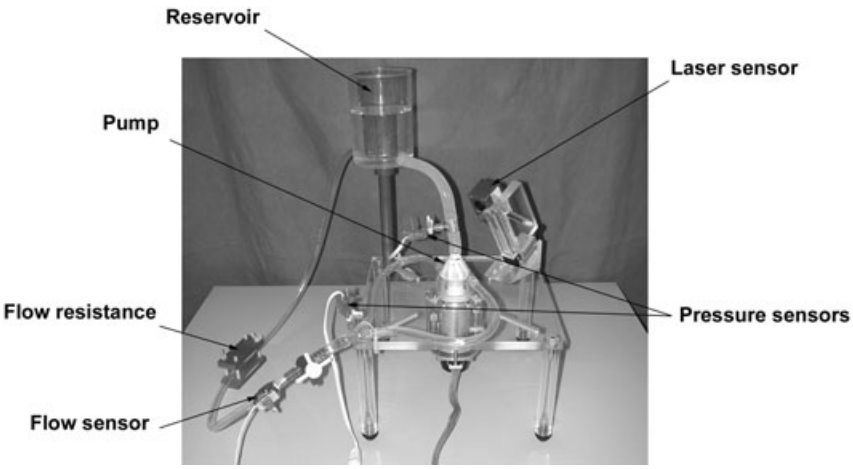

FIG. 3. Test setup used to investigate the hydrodynamic rotor behavior.

Numerical simulations

Numerical simulations were performed to optimize the rotor geometry and the pump efficiency. To generate the computational mesh, the software package Gambit 2.2 (Fluent, Inc., Lebanon, NH, USA) was used. The numerical simulations were performed with the Computational Fluid Dynamics (CFD) software package Fluent 6.2 (Fluent, Inc., Lebanon, NH, USA). A Dell Precision Workstation 670 with a 3.2 GHz dual-processor unit was used.

Blood was modeled throughout the simulations as a Newtonian fluid with a constant viscosity of 0.0035 kg/m·s and a constant density of 1020 kg/m^3. Because the flow was mainly turbulent, it was appropriate to use the "realizable k-ε model" with enhanced wall functions.

Due to the complex geometry of the rotor, the domain of calculation had to be limited. The simulation was carried out for one rotor vane, to estimate the flow distribution in the pump, and periodic boundary conditions (6) were used. At the pump inlet the flow velocity was fixed; at the outlet a constant static pressure was assumed (7).

Pump testing

The pump was tested in two steps. First, the rotor behavior was investigated purely mechanically to find pump settings that minimized vibration of the rotor and gave desirable running conditions. In the second step, the pump was tested to determine its rate of hemolysis, using pump settings in the range chosen during mechanical testing.

Hydrodynamic testing

The test stand used in this study is shown in Fig. 3. Because rotors in pumps of the type under development have relatively little mechanical constraint, special attention was paid to its movement. Rotor movement and vibration was measured optically with a Laser Triangulation Sensor (LTS)—Type R-LAS-L T-80_WA-ANA produced by Sensor Instruments GmbH, Thurmansbang, Germany. A housing manufactured out of transparent PMMA was used for these measurements to allow the laser beam to strike the rotor surface. This surface had to be highly reflective and was therefore coated with a thin layer of white paint (Type RAL 9010M, Shuller Eh'klar GmbH, Astenfeld, Austria). Flow was measured using an ultrasonic flow probe (Type HT 207, Transonic Systems, Inc., Ithaca, NY, USA). Pressure sensors (pvb, Critical Care GmbH, Kirchseeon, Germany) were used to measure the pressure changes generated by the pump.

The system was optimized with two adjustments, as shown in Fig. 4: the total gap, G_T between the inner cone and the outer housing, and the gap, G_I between the rotor and the inner cone. The gap, G_O that is outside the rotor is then $G_T - G_I$. G_T was set mechanically by changing the axial position of the inner cone. G_O and G_I are determined by the total gap (G_T), by the position of the magnet drive, and by the hydrodynamic forces. Under no-flow conditions, the magnets of the rotor and the magnet drive are aligned as dictated only by the magnetic forces. The position of the magnet drive that causes the rotor to be located exactly between the outer housing and the inner cone ($G_O = G_I$) was defined as the "no axial shift position." In the shifted condition, the magnet drive was moved toward the outer housing. This shift was measured starting from no axial shift position.

When the pump was started G_O increased (G_I decreased, respectively) because the hydrodynamic forces act downward in the sense of Fig. 4.

G_T was set in the range of 300 µm (0.3 mm) to 700 µm (0.7 mm), and G_O was typically set to near

Abbott v. Miracor, IPR2025-00116
Miracor Ex. 2022, p. 3 of 8

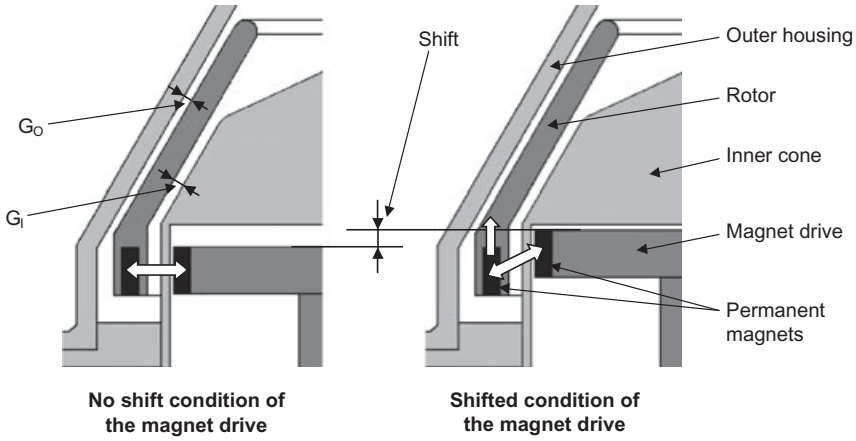

FIG. 4. Position of the rotor in the housing. G_O is the gap between the outer housing and the rotor. G_I is the gap between the rotor and the inner cone. G_O and G_I are determined by the position of the magnet drive and also by the hydrodynamic forces.

zero and increased during pump operation to values in the range of 50 µm (0.05 mm) to 250 µm (0.25 mm).

To effect exact positioning, micrometer heads (type MHK-15, Mitutoyo Corporation, Neuss, Germany) were used. Adjustments could be made to an accuracy of 0.01 mm.

For each rotor type, flows, pressures, and rotor vibration were observed.

Tests were performed for all three rotors at rotational speeds of 2000, 2500, and 3000 rpm at total gaps (G_T) of 0.3, 0.5, and 0.7 mm.

The pump characteristic curves were measured at fixed speeds and positions of the magnetic drive. Resistance in the tubing was increased incrementally until there was no flow. Pump characteristic curves with different axial positions of the magnetic drive were recorded. This position was varied in 0.1 mm steps. The possible total axial movement of the magnetic drive unit was about 1 mm.

The test fluid was a mixture of 40% glycerin and 60% water with a reported density of 1100 kg/m^3 and a viscosity 4×10^{-3} Pa·s at a temperature of 23°C (8). These values are comparable with those of blood under physiologic conditions.

Blood damage testing

In vitro hemolysis tests were performed in order to see if this pump concept could function at an acceptable level of blood trauma. To allow clear comparisons, a test methodology based on ASTM Standards F1830-97 and F1841-97 was used (9,10). A Biomedicus BP-80 blood pump (Medtronic, Inc., Minneapolis, MN, USA) served as a control device to nullify the sensitivity of the blood that was used. For these tests, Hemobear pumps made of PMMA with polished surfaces were used. When two pumps with different rotor designs were compared, they were tested simultaneously.

Porcine blood was obtained from a slaughterhouse, fresh for each study. The collection bags were prepared with 10 000 units of heparin and filled with 2.5 L of blood. The total priming volume of each mock circuit was 500 mL and the pumps were operated at 5 ± 0.25 L/min against an afterload of 150 mm Hg. In the hydrodynamic tests, the afterload was 180 mm Hg with these settings. The difference between the afterload pressure here and that in the hydrodynamic tests was caused by a different test setup. The blood temperature was kept at 37 ± 1°C, by placing the reservoir in a heated water bath. Blood samples of 2 mL were taken every hour until the test duration, about 5 hours, was reached.

RESULTS

Hydrodynamic behavior

Characteristic curves at three different rotor speeds: 2000, 2500, and 3000 rpm are shown in Fig. 5. Results for all three rotors and all settings are grouped because no significant difference in pumping

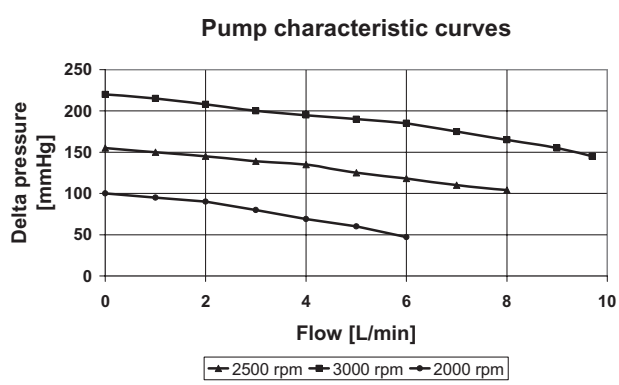

FIG. 5. Pump characteristic curves at different pump speeds. Data from all rotors are shown together because no difference among them was detected.

Abbott v. Miracor, IPR2025-00116
Miracor Ex. 2022, p. 4 of 8

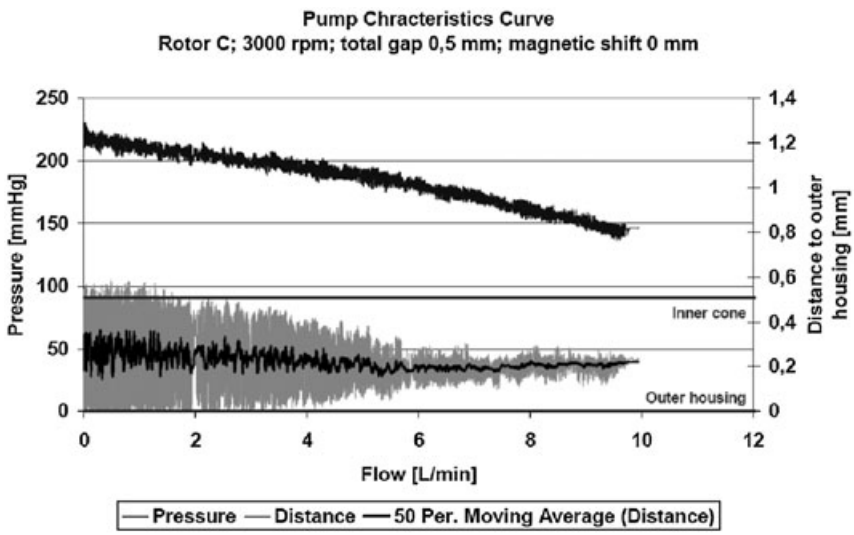

FIG. 6. Pump characteristics curve showing regions of unacceptable rotor vibration, obtained with no axial shift of the magnet drive unit. The left axis shows the pressure head. The right axis shows the distance between the rotor and the outer housing, which oscillated rapidly. The envelope of these oscillations is shown in gray, with a black line showing the moving average of 50 periods. The lines marked inner cone and outer housing show the calculated range of movement of the rotor within the pump. When the gray lines intersect these lines, the rotor makes contact with the housing.

performance among the rotors could be seen. With the magnetic settings used, it was not possible to increase rotational speed above 3000 rpm, because the torque was too high, and decoupling occurred.

It was found that the impeller can run stably over the operating range of flows and pressures shown on the figure. The pump requires rotational speeds of at least 2000 rpm to ensure proper behavior of the hydrodynamic bearing. The axial position of the magnet drive strongly influences rotor stability. With insufficient axial shift, the rotor cannot run stably over the whole flow range, high-amplitude oscillations are seen, and the rotor contacts the housing. Figure 6 shows a characteristic curve obtained under these undesirable conditions, with high vibration levels at flows lower than 6 L/min.

Axial shifting of the magnet drive sharply reduces these vibrations. Figure 7 shows the effect of shifting the magnet drive by 0.5 mm. With this setting, the rotor is slightly forced against the outer housing, so that during rotation this pretension is balanced by hydrodynamic forces, leading to stable flows. The rotor runs smoothly with low and uniform vibration over the whole flow range, at a separation, G_O of 0.1 mm from the outer housing and 0.3 mm (G_I) from the inner cone. Only vibration with a maximum movement of the rotor lower than 0.2 mm and no contact of the rotor with the housing over the whole flow range was considered acceptable.

The best running conditions, with lowest vibration of the rotor, were achieved at a rotational speed of 3000 rpm and a total gap of 0.5 mm, and these set-

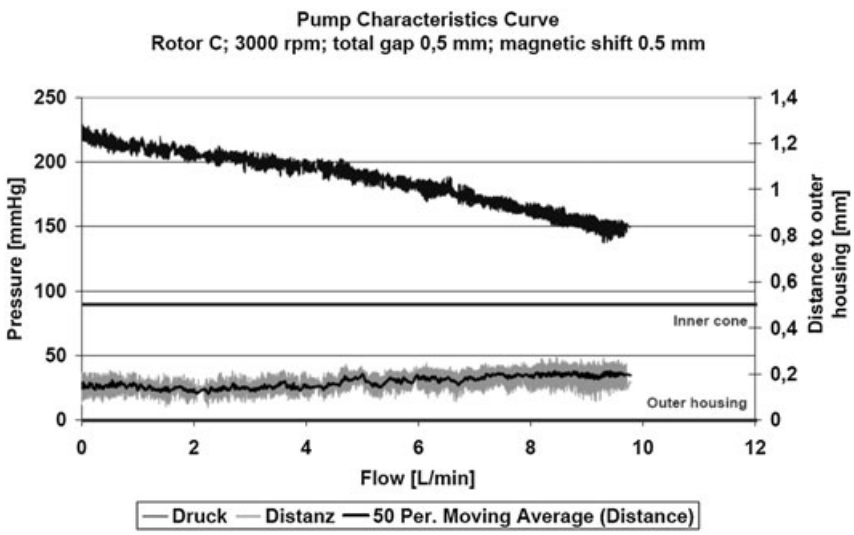

FIG. 7. Pump characteristics curve with 0.5 mm axial shift of the magnet drive unit. The rotor shows very low vibration.

Abbott v. Miracor, IPR2025-00116
Miracor Ex. 2022, p. 5 of 8

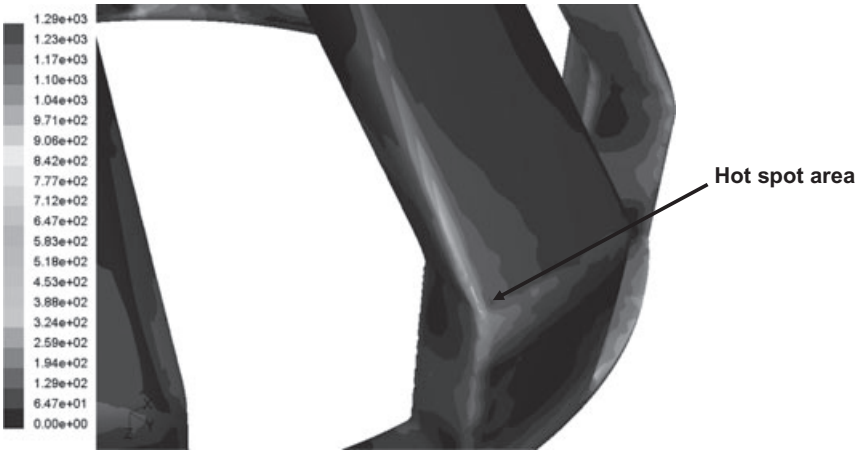

FIG. 8. Contours of wall shear stress on rotor A. A hot spot region exists on the leading edge.

tings were used for all further tests. At a total gap of 0.7 mm the working range is reduced and rotational speeds of at least 2500 rpm were found necessary. Oscillations of the rotor increased at low flow rates.

Numerical simulations

Simulations of rotor type A revealed a region of high shear, a so-called "hot spot," on the rotor vane, likely to cause blood damage (11). Figure 8 shows the contours of wall shear stress on rotor A in the "hot spot" region. The peak wall shear stress was calculated as 1293 Pa. On rotors of type B and C, these peaks were attenuated by increasing the rounding of the leading edge of the rotor vanes.

Figure 9 shows the influence of the position of the stabilizing ring. When the ring is placed on the bottom of the rotor, a stagnation zone exists, which can be seen on the left picture. If the ring is mounted on the inside the stagnation zone is eliminated. This position also reduces the maximum stagnation pressure, due to a better flow-through.

Hemolysis tests

Figure 10 shows the blood damage of the Hemobear pumps with different rotor types and different shifts of the magnet drive in comparison with the Biomedicus BP-80 pump. The Hemobear pumps were adjusted to the conditions previously established, using a total gap of 0.5 mm, a rotational speed of 3000 rpm, and magnetic shifts between 0.4 and 0.9 mm. The results demonstrate that rotor A, with the hot spot area found in the CFD simulations, creates relatively large blood damage (NIH = 0.014 ± 0.007 g/100 L, $n = 8$). The modified geom-

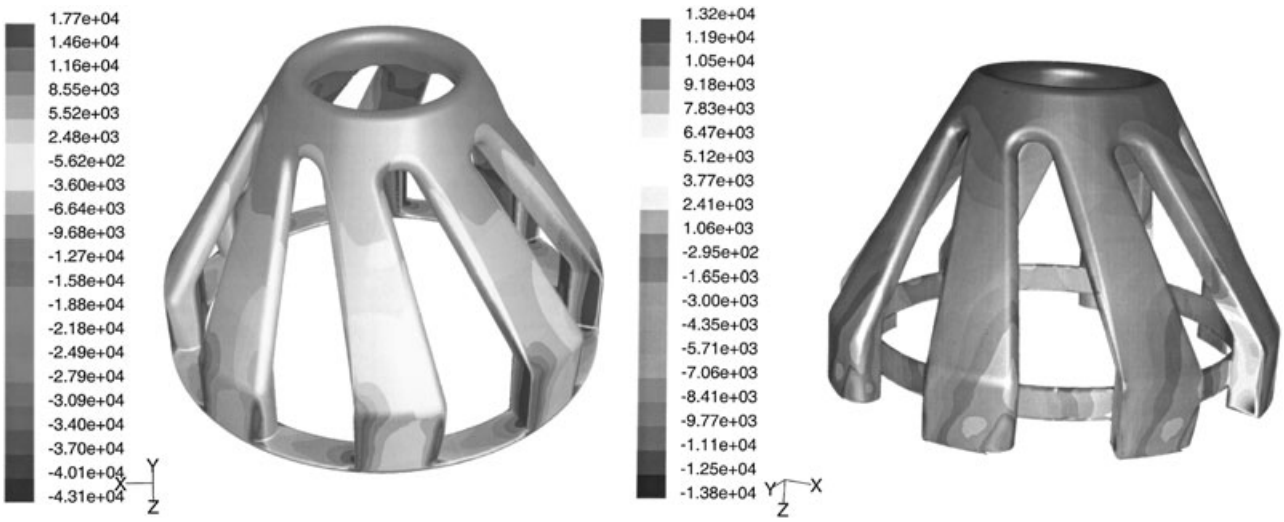

FIG. 9. Influence of the stabilizing ring on the static pressure of the rotor. When the ring is placed on the bottom of the rotor, a stagnation zone exists, which can be seen in the left picture. If the ring is mounted on the inside the stagnation zone is eliminated. This position also reduces the maximum stagnation pressure, due to a better flow-through.

Abbott v. Miracor, IPR2025-00116
Miracor Ex. 2022, p. 6 of 8

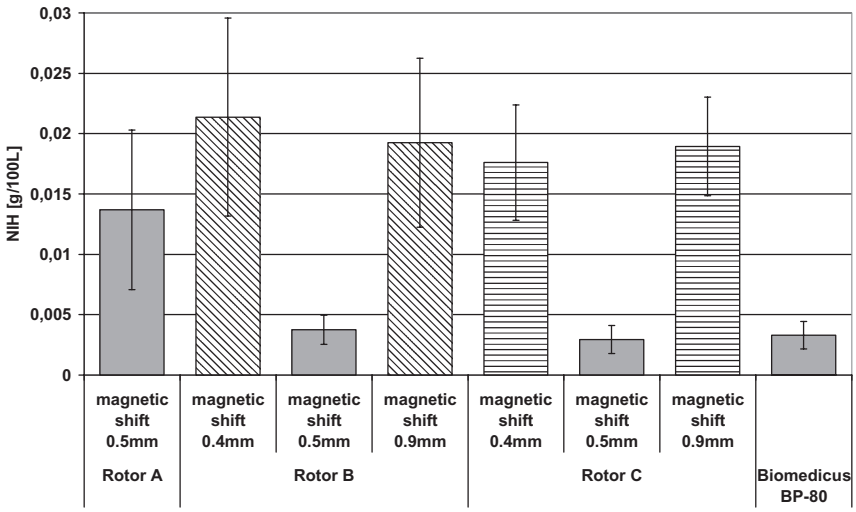

FIG. 10. Influence of the shift of the magnet drive on blood damage. The figure shows that rotor A is more hemolytic than rotors B and C, as predicted by CFD studies. The figure also shows that rotors B and C show minimum hemolysis at a magnetic shift of 0.5 mm, with values comparable with that exhibited by the BP-80 pump that was used as a control device in these studies. All data shown here were obtained at a flow rate of 5 L/min and an outlet pressure from the pump of 150 mm Hg.

etries of rotors B and C allowed blood damage to be reduced dramatically. Rotor B created a NIH value of 0.0038 ± 0.0012 g/100 L, $n = 2$ while the value for rotor C was 0.0029 ± 0.0012 g/100 L, $n = 5$.

Figure 10 demonstrates that the position of the magnet drive influences blood damage although low vibration levels persist. When the magnet drive is shifted 0.4 mm, the rotor pretension seems insufficient and increased blood damage is seen. When a shift of 0.5 mm is used, blood damage is reduced. When the shift is further increased, blood damage rises again.

The tests reported here clearly demonstrate that the Hemobear pump has low hemolysis and good hydrodynamic performance with critical adjustment of the magnetic drive. The blood damage is in the range of contemporary extracorporeal bearingless blood pumps, such as the Levitronix Centrimag blood pump whose NIH hemolysis index has been reported as 0.0029 ± 0.006 g/100 L (12). This is comparable with that observed for the Hemobear: 0.0029 ± 0.0012 g/100 L.

DISCUSSION

The study showed that the Hemobear concept can achieve good hydrodynamic performance at an acceptable level of hemolysis. However, a passive magnetic bearing operating at a large gap requires harmonization of the position of the rotor and the rotational speed. Large gaps encourage oscillation and small gaps encourage shear-induced hemolysis. In the present design, the rotor is repositioned by axial movement and the chosen value must respect the possibility of increased blood damage. The range, within which blood damage is low, is very small and has been defined so far only by direct measurements of blood damage. The hydrodynamic tests only define stability, but this is not enough information to predict the blood damage, because there is no information about the shear stress in the fluid gap. Any axial shift to achieve a desirable pretension must not be too high, because then blood damage increases due to higher shear stress in the fluid gap.

It was shown that CFD is a good tool for optimization of this pump. The CFD simulations highlighted a hot spot on rotor A, and this tendency was confirmed in experiments where this rotor showed highest blood damage. Lowest blood damage could be achieved with the modified rotor C with an axial shift of its magnetic drive by 0.5 mm. The shift of 0.5 mm produced low oscillation without excessive forcing of the rotor against the outer housing.

Direct, dynamic laser measurement of rotor behavior has not been previously reported for blood pumps. The technique is precise and was important in understanding pump behavior.

It was not the intention of this work to optimize the specification and placement of the magnets. Further work is needed both to stabilize normal operation, and startup and shut-down, as well as the response of the pump to external accelerations.

Nevertheless, because the total gap is in the range of 0.5 mm, comparably large manufacturing tolerances are possible. These should allow low-cost production using standard injection molding techniques. The absence of any need for electronic control of the rotor position removes an important failure mode and further reduces the estimated costs of production.

Abbott v. Miracor, IPR2025-00116
Miracor Ex. 2022, p. 7 of 8

CONCLUSIONS

A passive magnetically and hydrodynamically suspended rotary blood pump with a large total gap between rotor and housing has been realized. Hydrodynamic studies and CFD have been used to optimize the rotor geometry. With accurate adjustment of the magnet drive, low blood hemolysis is achieved, as proven by standard in vitro blood damage tests. The large-gap feature of this pump should allow higher manufacturing tolerances than other hydromagnetically levitated pumps and thus a production cost low enough to allow its use in disposable pump heads. Further work, primarily in the development of the permanent magnet drive, is needed to improve and insure stable operation.

Acknowledgment: The authors thank Professor Edward Leonard of the Department of Chemical Engineering, Columbia University, New York for reviewing the manuscript.

REFERENCES

1. Hoshi H, Shinshi T, Takatani S. Third-generation blood pumps with mechanical noncontact magnetic bearings. *Artif Organs* 2006;30:324–38.
2. Bearnson GB, Jacobs GB, Kirk J, Khanwilkar PS, Nelson KE, Long JW. HeartQuest ventricular assist device magnetically levitated centrifugal blood pump. *Artif Organs* 2006;30:339–46.
3. Watterson PA, Woodard JC, Ramsden VS, Reizes JA. VentrAssist hydrodynamically suspended, open, centrifugal blood pump. *Artif Organs* 2000;24:475–7.
4. Kink T, Reul H. Concept for a new hydrodynamic blood bearing for miniature blood pumps. *Artif Organs* 2004;28:916–20.
5. Reul HM, Akdis M. Blood pumps for circulatory support. *Perfusion* 2000;15:295–311.
6. Fluent Inc. Periodic boundaries. In *Introductory Fluent Notes*. Lebanon, NH: Fluent Inc., 2003;4–19.
7. Pirker S. CFD Untersuchung des Strömungsverhaltens in der "Hemobear" Blutpumpe. Johannes Kepler Universität Linz, Internal Report. 2004: 3–4.
8. Reindl C. Untersuchungen zu einer hydraulisch und magnetisch gelagerten Blutpumpe. Diplomarbeit an der Fachhochschule Technikum Wien. 2002.
9. ASTM. *F1841-97: Standard Practice for Assessment of Hemolysis in Continuous Flow Blood Pumps*. West Conshohoken, PA: American Society for Testing and Materials, 1997.
10. ASTM. *F1830-97: Standard Practice for Selection of Blood for In Vitro Evaluation of Blood Pumps*. West Conshohoken, PA: American Society for Testing and Materials, 1997.
11. Schima H, Müller MR, Papantonis D, et al. Minimization of hemolysis in centrifugal blood pumps: influence of different geometries. *Int J Artif Organs* 1993;16:521–9.
12. Zhang J, Gellman B, Koert A, et al. Computational and experimental evaluation of the fluid dynamics and hemocompatibility of the CentriMag blood pump. *Artif Organs* 2006;30:168–77.

Abbott v. Miracor, IPR2025-00116
Miracor Ex. 2022, p. 8 of 8